京都大学防災研究所年報 第 56 号 B 平成 25 年 6 月
Annuals of Disas. Prev. Res. Inst., Kyoto Univ., No. 56 B, 2013

Ocean Circulation Response to Inflow from Abukuma River Outlet

Josko TROSELJ(1), Yosuke YAMASHIKI(2) and Kaoru TAKARA

(1) Graduate School of Engineering, Kyoto University
(2) Graduate School of Advanced Integrated Studies in Human Survivability, Kyoto University

Synopsis

The focus of this study is to promote relevant modeling survey on Land-Ocean coupling modeling approach applicable for the bay and estuary zone affected by river inflow and associated pollution from the Abukuma river basin in Japan. The modeling approach has been studied by combining hydrological model and ocean circulation model (MSSG model, JAMSTEC) which runs within supercomputer (ES2), and associated data manipulation techniques for boundary conditions of hydrological and oceanographic modeling. There were simulated 3 different cases, at first circulation of ocean itself induced by its own temperature and salinity data differences, at second response of the ocean circulation to inflow from the river outlet, and finally response of the ocean to river inflow with included rotation of the Earth as Coriolis effect.

Keywords: ocean model, river inflow, coastal zone, integrated model, Coriolis effect

1. Introduction

Modeling of a contact zone between a river coming from potentially contaminated basin and an ocean is especially sensitive case for Land-Ocean mutual interaction due to significant risk of major environmental disaster which can occur in the case of contamination of the coastal zone. Therefore, it is of great importance to study and develop integrated modeling approach to comprehend the complex interaction processes in the contact zone in order to minimize disaster risk potential, which can consequently cause undesirable social and economical costs. Moreover, all land-induced activities influence the downstream catchment and related fishery production.

In order to gain appropriate computational modeling skills to comprehend the complex interaction processes in contact zone between a river and ocean, GCOE-HSE Advanced Capstone Project as a long term internship was undertaken at Japan Agency for Marine-Earth Science and Technology (JAMSTEC) in Yokohama for 10 weeks. It was studied a hydro 3-D integrated modeling approach of MSSG model, which combines coastal and river zones, in order to extend my research field into larger scale phenomena in Adriatic Sea affected by the river water intrusion, which will be a site study field for later part of my doctoral course.

Abukuma river outlet was considered as a sample site for the contact Land-Ocean zone, and the ocean circulation response to induced inflow from the river side was considered. I am planning to apply my knowledge into the similar catchment area in Croatia, particularly into Rijeka Metropolitan Region (RMR) and many bays along the Adriatic Sea coastline, in order to evaluate potential risk and security level for the downstream area.

2. Geographical position

The Abukuma river watershed is located in the northeast of Japan mainland, and has an area of 5,400 km^2 of which forest and agricultural land use accounts for 79% and 18% respectively. Most of the mainstream runs in the middle of the watershed from the south to the north. Many tributaries run eastward to westward. The headwater starts from Asahidake (elevation of 1,835 m) and reaches down the Pacific ocean. The elevation of the watershed ranges from the sea level to more than 2,000 m on the west side, where a volcanic mountain range is located. On the contrary, a peneplain is dominant on the east side of the mainstream, forming mountains of low elevation and gentle river slope (Kinouchi and Musiake, 2008). Figure 1 represents Abukuma watershed and two lakes located outside the watershed, and Photo 1 shows satellite image of Abukuma river mouth.

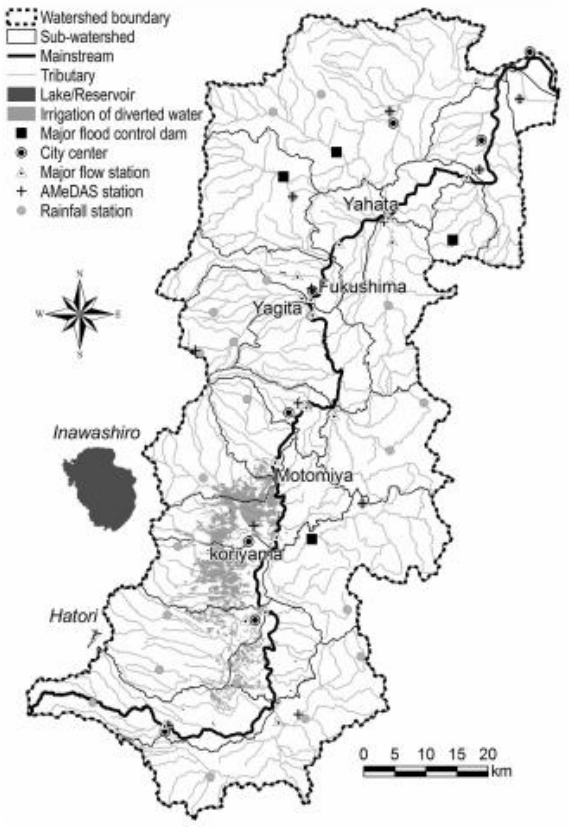

Fig 1 Abukuma watershed and two lakes located outside the watershed (Kinouchi and Musiake, 2008)

Photo 1 Abukuma river mouth satellite image (Adityawan et al., 2012)

3. Model Description

ETOPO1, 1 Arc Minute Global Relief Model was chosen as initial database for bathymetry data, while World Ocean Atlas 2005 dataset was chosen as initial 3D database for temperature, salinity, pressure, and velocity field data. The ocean model was set up rectangular with 200*200 cells with resolution of 300 meters, 60 km range in longitude axis with 1 day output data for ocean only, and 1 hour output data increment for river input, starting from 1st of June 2005. River outlet was positioned on the central west point of the model. In order to simplify the model physics, the ocean depth was set flat at 52 meters depth with layers of 1 meter increments, which is sufficiently deep so that river plumes never touch the seafloor (Isobe, 2005). The river side boundary conditions were simulated by extending the model bathymetry throughout the river mouth at 38.05 N latitude, with constant 1200 meters width and 7 meters depth, and the river flow input was set to 1300 m^3/s with uniform velocity distribution over the cross section at the entrance point on the central west side of the domain. The upper, lower and right borders of the domain have remained closed. Finally, it was simulated additional boundary condition into the model, which included existence of the Coriolis effect.

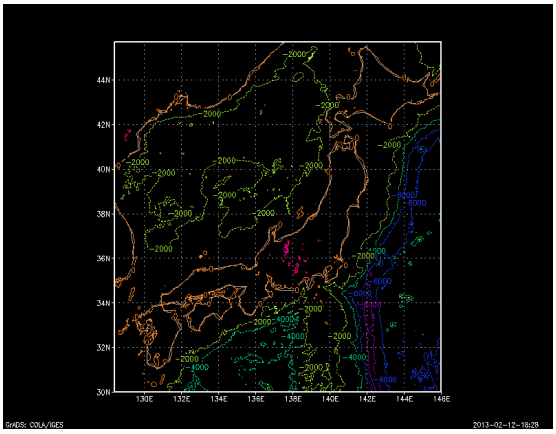

Fig 2 Barometry of Japan adjacent area [m]

Barometry data of Japan adjacent area from ETOPO1 (Amante, Eakins, 2009) dataset are presented in Figure 2. It was chosen mainly because its surveys were collected by several various ocean research Institutes which revisited limited number of localities during surveys, and surveys were done with the most modern technology by using GPS navigation Acoustic Doppler Current Profiler (ADCP) and databases were integrated together and smoothed in order to prevent improper steps, so working with that type of dataset was very simple and reliable.

World Ocean Atlas 2005 (NODC, 2007) dataset was chosen as 3D database for temperature, salinity, pressure, and velocity field data mainly because surveys for the database were done in situ and it contains many various statistical analyses, as well as available basic sources of all calculations of datasets. The database was made for 33 standard depths from ocean surface to depth of 5,500 meters.

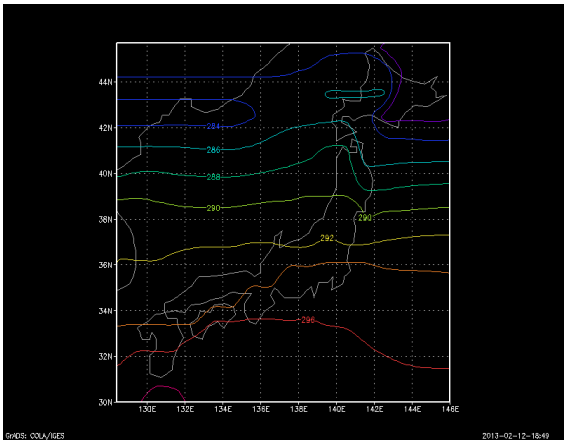

Fig 3 Temperature data of ocean surface level of Japan adjacent area (01/06/05) [K]

Fig 4a Position of the model

Temperature data on ocean surface layer of Japan adjacent area for 1st of June 2005 are presented in Figure 3. Figures 4a and 4b represent position and domain for the model, with red line on Figure 4b representing direction of river inflow perpendicular to direction of coastline in the river mouth.

Fig 4b Domain of the model (Google Earth, 11th of February 2013)

3.1 Model equations and methodology

The model is operating by using Navier Stokes equation (1).

$$\rho\left(\frac{\partial \mathbf{v}}{\partial t}+\mathbf{v}\cdot\nabla\mathbf{v}\right)=-\nabla p+\mu\nabla^2\mathbf{v}+\mathbf{f} \qquad (1)$$

With simplifications gotten from using finite elements method, the equation (1) can be transformed into equation (2).

$$v(t_2) = v(t_1) - v\nabla v - (\nabla\ p - \mu\ \nabla^2 v)/\rho + f/\rho \qquad (2)$$

This equation represents temporal changing of velocity field data simulated by the model. After setting up initial conditions for the model, it have been continuously improved by adding more boundary conditions, in order to increase precision of simulated results and to get more reliable output data. It is done by changing the "f" variable of the equation, which represents external influences to the hydrodynamic physical processes. Adding more complex boundary conditions are next steps in my doctoral study.

Initial conditions of velocity field were static, and ocean was in non equilibrium quasi stationary state. Fluid circulation was induced for 3 different initial conditions, one when ocean circulation was induced by its own temperature, salinity and pressure differences among adjacent cells, second when initial side boundary conditions from river side inflow was simulated together with self induced ocean, and the most advanced initial conditions when external factor of the Earth rotation was put into the simulation. Equation (3) proves that the ocean with given initial conditions are in non equilibrium quasi stationary state, while Figure 5 schematically presents how the circulation of ocean is transformed from that state into dynamic state.

$$\begin{aligned}&Ep + Ek = const;\\ &t=0:\ Ep_1 + Ek_1 = Ep_2 + Ek_2\ ;\ Ek_1=Ek_2=0\\ &\rho_1 gh = \rho_2 gh;\ \rho_1 = \rho_2 \rightarrow \text{Equilibrium state}\\ &\rightarrow\ T_1 \neq T_2,\ sl_1 \neq sl_2 \rightarrow \rho_1 \neq \rho_2\\ &\rightarrow \text{Quasi stationary non equilibrium state}\end{aligned} \qquad (3)$$

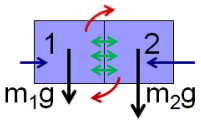

Rotation, Translation, Diffusion

Fig 5 Scheme how the ocean circulation process is induced

The principle of available potential energy describes mechanism of physical processes for inducing the ocean circulation process, by using energy conservation principle, as it is described in equation (4), where $Ep_{(\rho \neq const)}$ is available potential energy, ρ^0 steady potential density (baroclinic stability) and ρ' available potential density which causes baroclinic instability.

$$Ep_{(\rho \neq const)} = \rho^0 gh + \rho' gh \qquad (4)$$

The circulating system inside closed borders will always tend to have uniform distribution of temperature, salinity and pressure data, in which case it would stop circulating. However, even with small domain like this and relatively small differences of initial data among cells, it was made rough estimation that the ocean induced by its own data differences would circulate for more than 10 years before spending all available potential energy gotten from the density differences.

3.2 Model set up and results, ocean itself

In addition to already mentioned initial data, initial bathymetry data were also provided as initial conditions for the model, as shown in Figure 6.

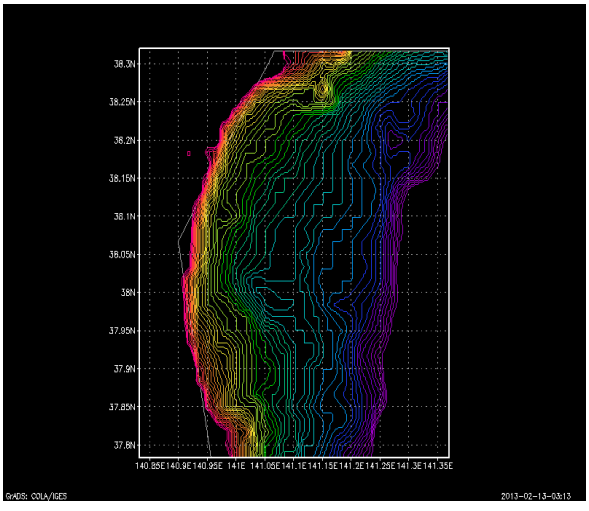

Fig 6 Initial bathymetry conditions [m]

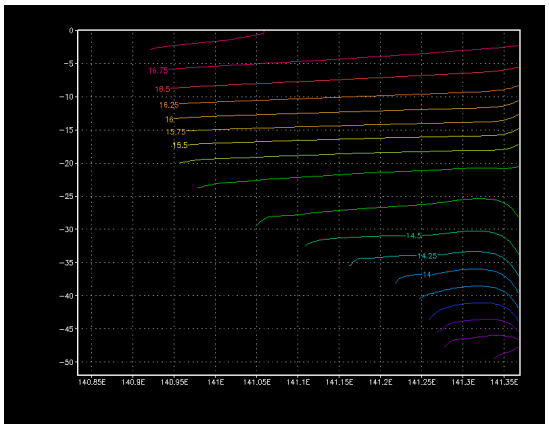

Fig 7a Longitudinal section of temperature data at 38.05 latitude, 5 days after starting itself induced ocean simulation [˚C]

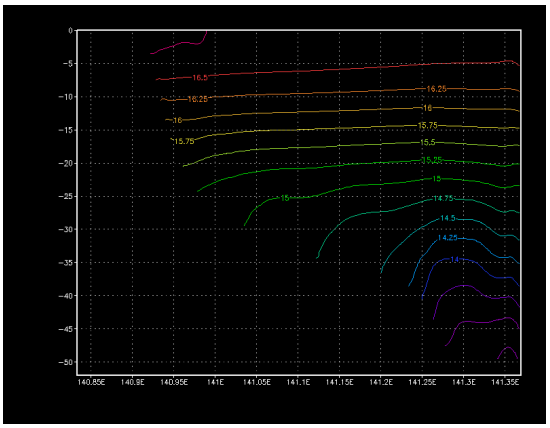

Fig 7b Longitudinal section of temperature data at 38.05 latitude, 30 days after starting itself induced ocean simulation [˚C]

The itself induced ocean simulation were run by 30 days of simulated time. It was optimal simulation time for chosen domain size. Results showed that it is enough time to induce ocean to circulate in relatively steady dynamic phase, which was one of my concerns before running the model. In this work I will present results of simulations which I found the most interesting among all available output data. Figure 7a shows longitudinal section of temperature data at 38.05 latitude 5 days, while Figure 7b shows it 30 days after the initialization of ocean circulation process.

3.3 Model results, ocean + river

After checking that itself induced ocean simulation is producing expected and reasonable results, river side boundary conditions were put into the model, as described earlier in this chapter. My primary focus during the research was gaining computational skills to be able to navigate inside the MSSG code and modify my input, so I was not spending a lot of time in analyzing exact conditions from the Abukuma river and therefore the estimation of river conditions was done roughly and simplified according to the information given from references (Matsumoto, 1981 and Yustiani, Mano, 2004). In upcoming part of my research I will change side river boundary conditions to be more realistic like on the site study. Figure 8a shows longitudinal section of salinity data for river domain at 38.05 latitude 4 hours, while Figure 8b shows it 11 hours after the initialization of the simulation. I wanted to get output data about length of ocean's water intrusion into river mouth and

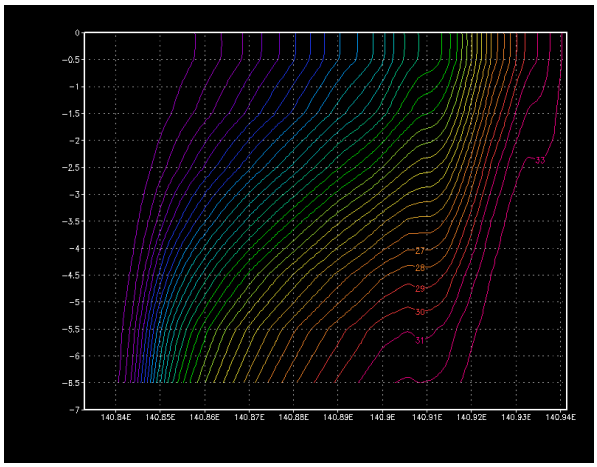

Fig 8a Longitudinal section (river domain) of salinity data at 38.05 latitude, 4 hours after starting the river simulation [‰]

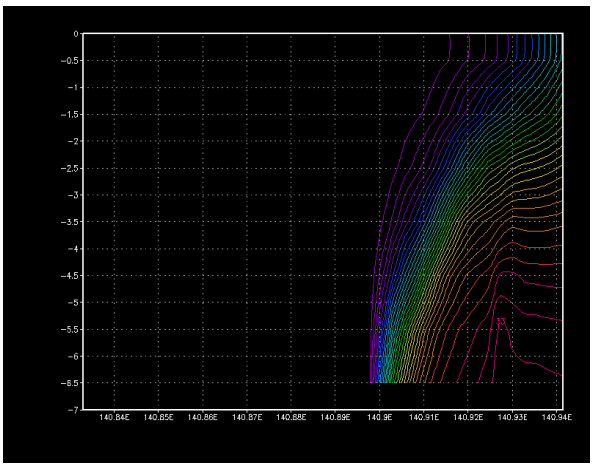

Fig 8b Longitudinal section (river domain) of salinity data at 38.05 latitude, 11 hours after starting the river simulation [‰]

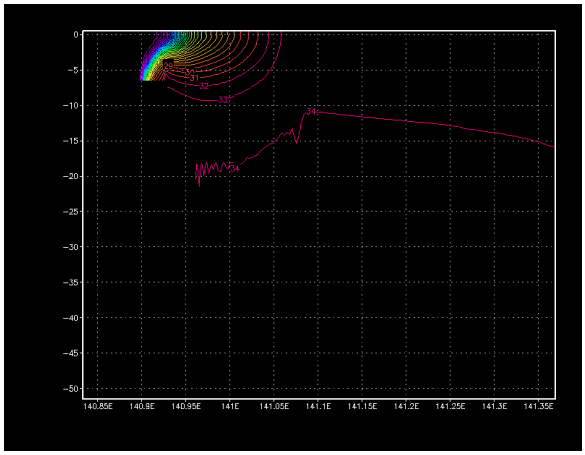

Fig 9a Longitudinal section (global domain) of salinity data at 38.05 latitude, 22 hours after starting the river simulation [‰]

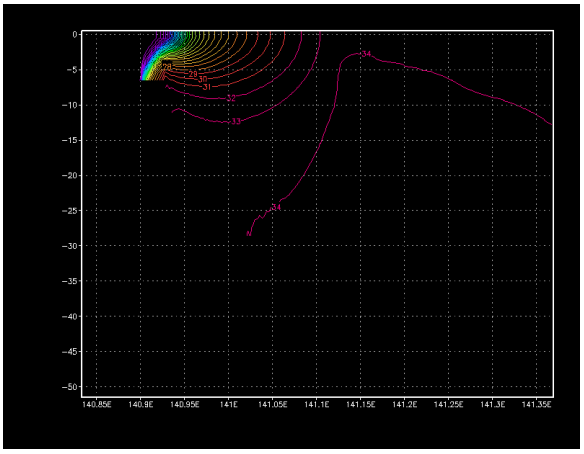

Fig 9b Longitudinal section (global domain) of salinity data at 38.05 latitude, 44 hours after starting the river simulation [‰]

therefore had chosen longer distance of river flow from coastline side than in real conditions. At the beginning, it was filled by ocean water with salinity of around 34‰, while river water salinity was set up as 0‰, and I was considering salinity gradient during time throughout the river channel until it became more or less uniform, which was sign that it has reached steady stage of mixing waters for the given conditions. The data after 4 hours the best represent period when river water overcame the river mouth, and effect of bottom friction which occurs by the way. The data after 11 hours represent the beginning of more or less steady salinity gradient at the position, so it represents real contact zone between river and ocean water which will be occurring during the whole process of the simulation. It is also interesting to notice position of the river water which repressed brackish water very close to the river mouth, which was logically to expect due to extremely high river flow used as a boundary condition. It would be interesting to see level of intrusion of brackish water for different border conditions, which will be one of concerns of my future study. Figure 9a shows longitudinal section of salinity data for global model domain at 38.05 latitude 22 hours, while Figure 8b shows it 44 hours after the initialization of the simulation. It can be seen that relatively steady phase of the brackish water body will be held during the whole time of the simulation. The ocean + river model successfully simulated 76 hours of data.

3.4 Model results, ocean + river + Coriolis effect

So far this simulation is the most advanced part that I reached during my doctoral study. As salinity is factor which has the biggest value's difference between ocean and river waters, I often used it as the most valuable indicator about directions of trajectories of the river water movement. Therefore, the salinity output data as the best indicator of influence of the Coriolis effect can be seen at Figures 10, presented on ocean surface layer 24 hours (Fig. 10a) and 48 hours (Fig. 10b) after inducing the simulation.

4. Conclusions and follow up

My main concern was about time of putting side boundary river inflow into the ocean model, because some time is needed until an ocean reaches its steady stage of circulation. While analyzing the ocean circulation output data, the direction which I was tending to search for was putting river inflow into the model on the time when ocean was already running for some time period by itself. Therefore, my goal was trying to simulate much closer natural conditions where an ocean response is occurring to an river inflow during initial dynamic stage for ocean and static stage for river inflow, and not during initial static stage for both which was simulated in this work. Finding computational solution in the model which will solve this problem is one of my major goals for upcoming research.

I was searching for conditions when it can be

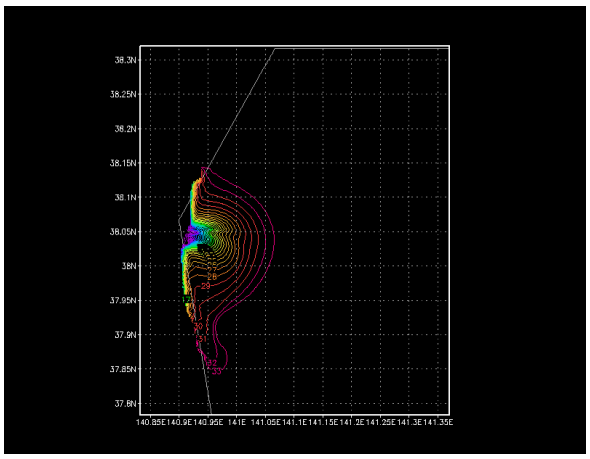

Fig 10a Salinity data on ocean surface layer, 24 hours after inducing the simulation with both river inflow and Coriolis effect [‰]

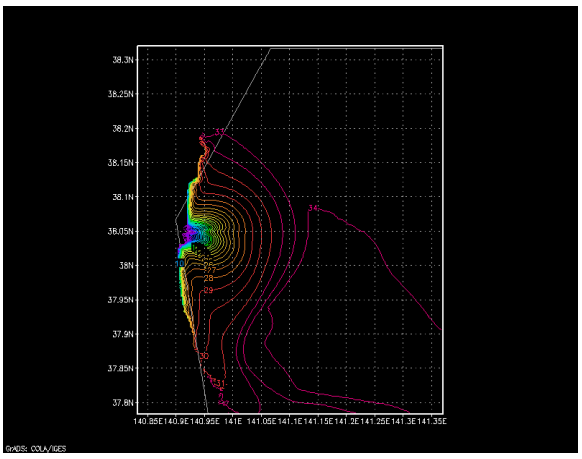

Fig 10b Salinity data on ocean surface layer, 48 hours after inducing the simulation with both river inflow and Coriolis effect [‰]

concluded that the ocean reached its steady stage of circulation. By my assumptions, the range between minimal and maximal elevation can be good indicator of that. When the range reaches more or less constant value, then it can be concluded that the ocean circulation has reached its steady stage. By following that assumption, I made analysis of maximal and minimal ocean surface elevation, as well as range between them in every time increment, as it is shown in Figure 11. It can be concluded that from 9th day after initialization the ocean reaches its steady stage for the current initial conditions and this kind of test. As ocean had initial velocity field zero, its movement was induced only because of temperature and salinity differences among adjacent cells. Density among adjacent cells was not the same because of the temperature and salinity differences, and therefore nor energy field was the same, which caused instability and initially induced movement among cells. A cell which has higher density will have higher mass than the one with lower density because volume of every cell is the same at the beginning. The cell with higher mass will be induced by higher gravity force as well as higher pressure force, which will produce rotational moment of the force around mid plane between two adjacent cells induced by gravity force, as well as translational movement of the cells in direction of higher pressure force, the process which will be repeated in every time increment. Figures 12 represent free ocean surface elevation at the first (Fig. 12a), fifth (Fig. 12b) and twenty-fifth (Fig.

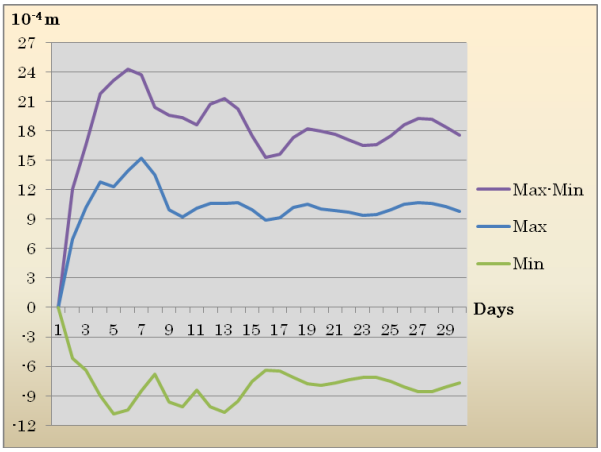

Fig 11 Maximal and minimal ocean surface elevation, and their mutual range for itself induced ocean model [m]

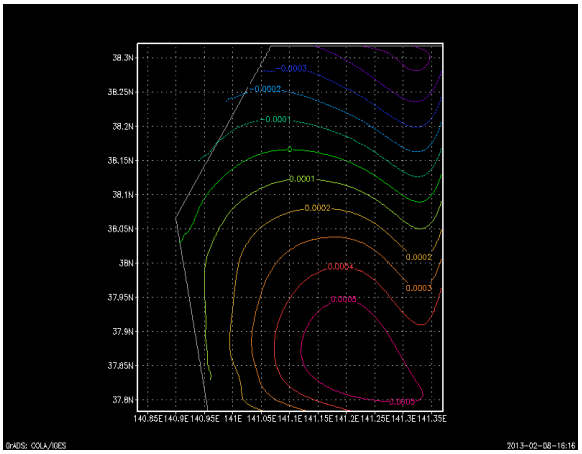

Fig 12a Ocean surface elevation, 1 day after inducing the ocean itself circulation [m]

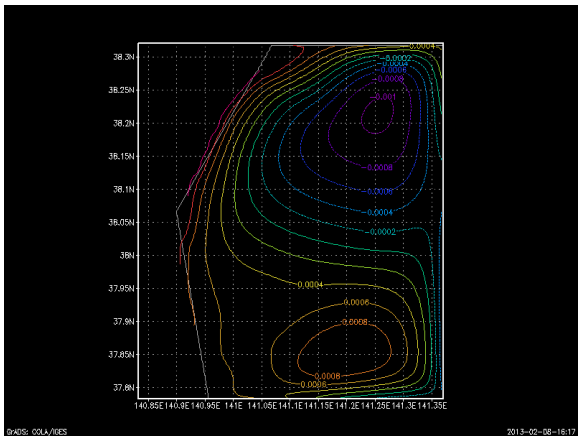

Fig 12b Ocean surface elevation, 5 days after inducing the ocean itself circulation [m]

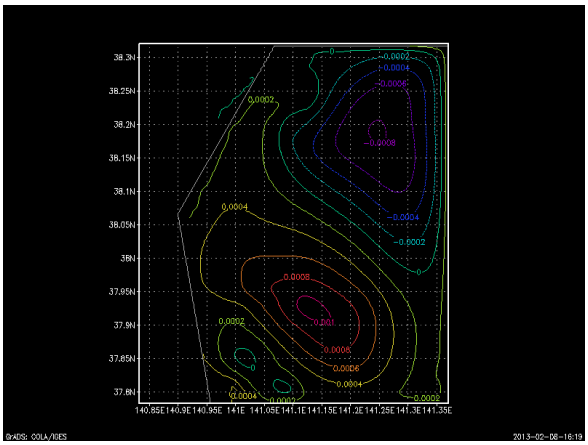

Fig 12c Ocean surface elevation, 25 days after inducing the ocean itself circulation [m]

12c) day after inducing the ocean movement.

The other main concern of special interest for me was momentum conservation principle. Following that principle, every force which is induced due to temperature and salinity differences among adjacent cells will also produce a counter force on the same line but in the opposite direction. The important conclusion following this is that total sum of rotational moments of every force in the system around every point will be zero, because initial conditions were related to static ocean and there was not any external force entering into the model, and the induced forces and counter forces will always produce the same value but the opposite angle of rotational moment around every point in the system. The principle becomes much more complicated when side boundary river input is added to the system, because it induces continuous force of water body uniformly distributed at the place of its appearance. Because of the fact that it is uniformly distributed, it can be concluded that there exists one line in the system, in the middle point of the river input, where sum of rotational moments of the whole system in every time increment will be zero. I am not sure if this conclusion is correct, but that is idea which came to my mind based on previous assumptions, and is for sure something where my future research will be directed. In order to find some evidence proving this principle, I made analysis of total sum of velocity directions for the available output data, and my expectations were that total sum of both x and y direction velocities will be around zero, with a little deviations because of vertical mixing of the ocean water which was not considered in this observation as well as ocean surface elevations, so not every time the same velocity gradient produces the same force because of the existing mass gradient between adjacent cells. Figure 13 represents results of the total sum of x and y velocities during time inside the whole system for the ocean model itself. It mostly showed results of less than 3 millimeters per second, which is negligible value in comparing with total size of the system. The mass conservation principle test was also done, and it showed average elevation of ocean surface layer of $1{,}31*10^{-4}$ m over 77,53% of cells which had water level data, which is equivalent to $3{,}65*10^{5}$ m^3 of water. It is only 0,13‰ of the total volume, which is added to the surface layer just at the time from first to second

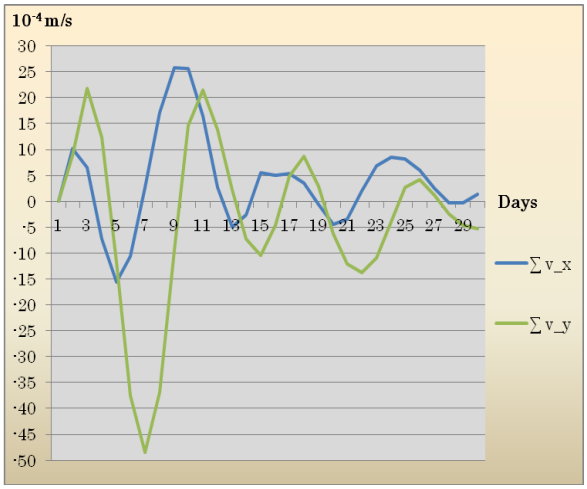

Fig 13 Total sum of x and y velocities inside the whole system for ocean model itself

time increment of the modeling. On every following time increments, elevation remains constant which proves that mass conservation principle is consistent. The starting lifting of the water level data can be explained with numerical model error, because the model itself also makes an calculating error when moving from static to dynamic phase of the ocean circulation. One of my concerns for upcoming research will for sure be including integrated 3D tests of the conservation principles instead of doing it in 2D level.

For ocean itself model, average surface temperature was reduced from 17.05 to 16.65 ˚C while the average bottom temperature was increased from 13.02 to 13.40 ˚C in the range of 30 days. Average ocean surface salinity in the same timeframe was increased from 33.88 to 33.92 ‰, while average bottom layer salinity was decreased from 34.23 to 34.21 ‰.

Acknowledgements

This research is part of Ph.D. study of the first author, which is supported by Ministry of Education, Culture, Sports, Science and Technology - Japan (MEXT). It is continuous research started as long term internship in Japan Agency for Marine-Earth Science and Technology (JAMSTEC), which was supported by Global Center for Education and Research on Human Security Engineering for Asian Megacities (GCOE-HSE) program.

I would like to express my honest gratitude to Professor Dr. Yosuke Yamashiki for initializing process of my application for the internship and for providing me with all technical support and advices which I needed during the time, GCOE-HSE program leaders for providing logistical support for the internship, Dr. Keiko Takahashi, program director of the MESSAGE model for accepting my application to complete the internship in JAMSTEC, as well as Dr. Shinichiro Kida to be my executive supervisor in behalf of JAMSTEC. They all, together with my Kyoto University supervisor Dr. Kaoru Takara, made significant contribution to my education progress.

References

Adityawan, M.B., Roh, M., Tanaka, H., Farid, M. (2012): The Effect of River Mouth Morphological Features on Tsunami Intrusion

Amante, C., Eakins, B.W. (2009): ETOPO1 1 Arc-Minute Global Relief Model: Procedures, Data Sources and Analysis, NOAA Technical Memorandum NESDIS NGDC-247, 19 pp

Isobe, A. (2005): Balooning of River-Plume Bulge and Its Stabilization by Tidal Currents, American Meteorological Society

Kinouchi, T., Musiake, K. (2008): Simulating hydrological impact of environmental change in the Abukuma Watershed, Japan, 4th APHW Conference

Matsumoto, H. (1981): Developmental Process of Alluvial Coastal Plain related to the Holocene Sea-level Change, The Science Reports of Tohoku University, 7th series (Geography), Vol 31, No. 2

National Oceanographic Data Center (NODC, 2007)

Yustiani, Y.M., Mano, A. (2004): Flood Effect on Nutrient Distribution in Open Coastal Waters off the Abukuma River, Asian and Pacific Coasts 2003: Proceedings of the 2nd International Conference, Makuhari, Japan

(Received June 11, revised version July 26, 2013)